Thermal Emission Spectrometer Mosaics Of Impact Craters: Progress on Shocked Plagioclase Detections.
J.R. Johnson, M.I. Staid, T.N. Titus, and L. Gaddis, U.S. Geological Survey, 2255 N. Gemini Dr., Flagstaff, AZ 86001, jrjohnson@usgs.gov.

***Introduction*:** High shock pressures disorder the mineral lattice of plagioclase feldspars and cause weakening and shifts in thermal infrared absorption bands related to an increase in diaplectic glass content, particularly at shock pressures above ~20-25 GPa [1-9]. We are continuing our investigation of spectral deconvolutions of TES mosaics and mosaics using standard TES orbits for eight impact crater areas. Using a combination of mineral laboratory spectra and spectra of experimentally shocked bytownite feldspars [5] to deconvolve the TES spectra, we find that locations of shocked feldspar detections are not restricted to ejecta near large craters.

Methodolgy: TES data. As part of the MGS Guest Observer Program, we requested TES mosaics of ejecta blankets associated with eight fresh impact craters > 50 km diameter in low albedo regions (e.g., Cimmeria Terra; Figure 1). Of the six TES mosaics acquired thus far all were acquired in 5 cm^{-1} mode, which we are binning to 10 cm^{-1} resolution for ease of analysis and comparison to 10 cm^{-1} data from single TES orbits (and any serendipitous 10 cm^{-1} mosaics; Figure 2). TES values for each detector footprint were replaced by the average values of each six-detector observation, and ISIS software was used for geometric projections of the TES data and MOC images [10-11].

Methodolgy: Deconvolutions. We revised the multiple endmember mixing approach used previously [6]. The algorithm still uses a spectral library composed of six atmospheric spectra [e.g., 12] combined with laboratory measurements of 40 minerals, glasses, and palagonitic soils, plus 10 spectra of anorthosite shocked to 17-56 GPa [cf. 7-13]. The current algorithm initially compares all possible ten-endmember combinations consisting of three laboratory spectral library components, the six atmospheric endmembers, and a blackbody. The blackbody is used to compensate for grain size variations between the library spectra and the TES spectra. The best model containing positive endmember abundances for each input spectrum is identified on the basis of the rms error computed for each combination. Then each unused library endmember is alternately added to the ten endmembers and a new rms error is calculated. The spectrum that provides the best improvement (and is selected with a positive abundance for all endmember components) is then kept as an additional endmember. If no additional spectrum results in all positive fractions and an improved error, the previous best solution is kept. This procedure is then repeated until as many as 12 mineral endmembers are selected. The algorithm produces fractions for each member chosen from the spectral library and a blackbody component. We run the algorithm over the spectral range 233-509 cm^{-1} and 827-1304 cm^{-1} with and without inclusion of the shocked anorthosite spectra [5]. Derived mineral abundances were normalized to 100%, and the results for common mineral groups were summed.

Results. Deconvolution results for the area in Figure 1 demonstrate that plagioclase, pyroxene, and olivines are most prevalent in the southern, lower-albedo region, whereas weathering products (clays, oxides) tend to occur in the northern, more dust-covered regions. Shocked anorthosites are identified at normalized abundances of 10-40%, although their distribution is not restricted to the large crater ejecta in Figure 1. Mosaics acquired within the northeastern ejecta and rim of the main crater at both 10 cm^{-1} (Figure 2) and 5 cm^{-1} (Figure 3) also show shocked feldspars, some of which appear correlated with ejecta features. However, more detailed comparisons of deconvolution results among these data sets are needed. Although rms errors suggest the deconvolution algorithm provides good fits to the TES spectra (Figures 1-3), further exploration of the parameter space in the spectral deconvolutions (and incorporation of TES data from other regions) is necessary to discern better the distribution of shocked feldspars on Mars.

***References*:** [1] Stöffler, D., *Forschr. Miner.* , 49, 50-113, 1972; [2] Stöffler, D., and F. Langenhorst, *Meteoritics,* 29, 155-181, 1994; [3] Ostertag, R., *JGR*, 88, B364-B376, 1983; [4] Gibbons, R.V., et al., *Proc. Lunar Sci. Conf. 6th,* 3143-3171, 1975; [5] Johnson, J.R., et al., *JGR,* 107(E10), doi:10.1029/2001JE001517, 2002; Johnson, J.R., et al., submitted to *Amer. Mineral.*, 2003; [6] Johnson , J.R. et al., LPSC XXXIII, #1345, 2002; [7] Thompson, J., and J. Salisbury, *Remote Sens. Environ.*,45, 1-13, 1993; [8] Ramsey, M.S., and P.R. Christensen, *JGR*, 103, 577-596, 1998.; [9] Staid, M.I., et al., Fall AGU abstract, 2001; [10] Titus, T. and H. Kieffer, in *Exploring Mars with TES: A data users' workshop*, Arizona State University, 2001; [11] Gaddis et al., this issue; [12] Bandfield, J.L., *JGR*, 107(E6) doi:10.1029/2001JE001510, 2001; [13] Sabol, D.E. et al., *JGR*, 97, 2659-2672, 1992; [14] Ruff and Christensen, *JGR*, 107(E12),10.1029/2001JE001580, 2002.

Acknowledgments. Thanks to K. Bender and K. Murray (ASU) for assistance with acquisition of TES mosaics, and J. Bandfield (ASU) for help with deconvolution techniques. This work was supported by the Mars Global Surveyor Data Analysis and Guest Observer Programs.

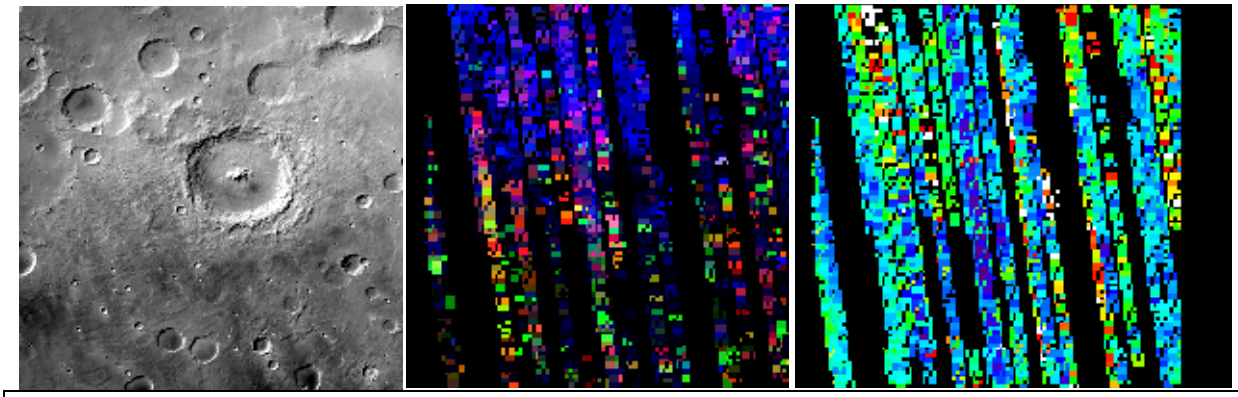

Figure 1. (***left***) Moc WA mosaic centered on –25º, 166ºE. Crater is 95 km diameter; (***middle***) pseudocolor image showing deconvolution results using shocked feldspar spectra in endmember library: RED = summed abundance of all shocked feldspar detections (10-40%); GREEN = average shock pressure levels for each pixel in which shocked feldspar was detected (17-56 GPa); BLUE = inverse of surface dust index (1.03-1.05) [14]. Blue areas are relatively dust-covered; red areas are high abundances of shocked feldspar but low shock pressures; green areas are low abundance of shocked feldspars but high pressures. Distribution of shocked feldspars is not restricted to the large crater's ejecta blanket; (***right***) rms error from deconvolution runs (0.001 (blue) to 0.004 (red/white)).

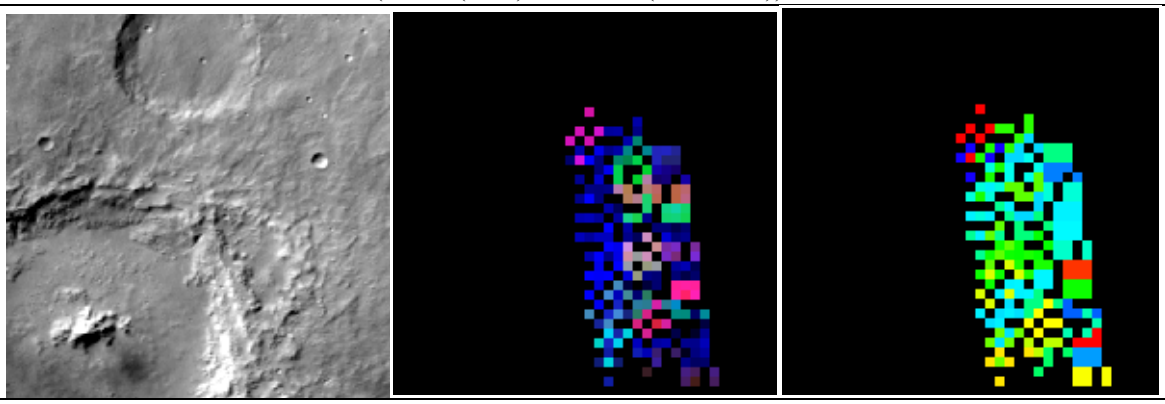

Figure 2. (***left***) Moc WA mosaic centered on –24º, 167ºE; (***middle***) pseudocolor image showing deconvolution results using 10 cm^{-1} mosaic (only partial coverage available in this mosaic); same color scheme used as Figure 1 but with inverse dust index displayed from (1.01-1.05); (***right***) rms error from deconvolution runs (0.001 (blue) to 0.003 (red)).

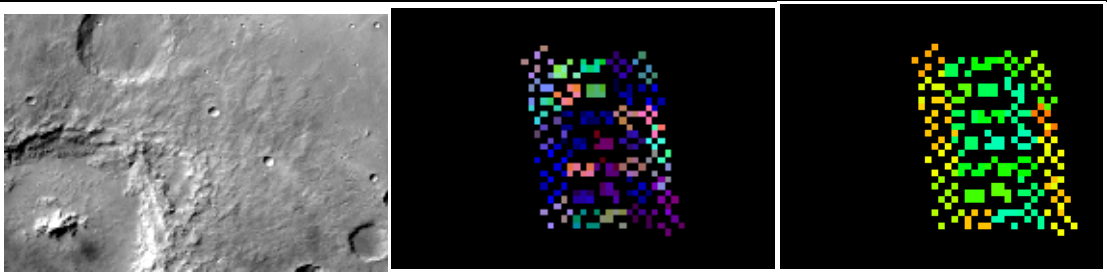

Figure 3. (***left***) Moc WA mosaic centered on –24º, 167.5ºE; (***middle***) pseudocolor image showing deconvolution runs using 5 cm^{-1} mosaic (convolved to 10 cm^{-1} resolution) ; same color scheme as Figure 1 but with inverse dust index displayed from (1.03-1.07); (***right***) rms error from deconvolution runs (0.001 (blue) to 0.004 (red)).